Friction
https://doi.org/10.1007/s40544-022-0709-3
ISSN 2223-7690
CN 10-1237/TH
RESEARCH ARTICLE

Tribological behaviour of $Ti_3C_2T_x$ nano-sheets: Substrate-dependent tribo-chemical reactions

Alberto ROTA[1,2,3,*], **Nicolas BELLINA**[3], **Bo WANG**[4], **Andreas ROSENKRANZ**[5]

[1] *Dipartimento di Scienze Fisiche, Informatiche e Matematiche, Università di Modena e Reggio Emilia, Modena 41125, Italy*

[2] *CNR- Istituto di Nanoscienze, Centro S3, Modena 41125, Italy*

[3] *Centro Interdipartimentale per la Ricerca Applicata e i Servizi nel settore della Meccanica Avanzata e della Motoristica, Università di Modena e Reggio Emilia, Modena 41125, Italy*

[4] *Key Laboratory of Marine New Materials and Related Technology, Zhejiang Key Laboratory of Marine Materials and Protection Technology, Ningbo Institute of Material Technology & Engineering, Chinese Academy of Sciences, Ningbo 315201, China*

[5] *Department of Chemical Engineering, Biotechnology and Materials, University of Chile, Santiago 8370456, Chile*

Received: Received: 03 May 2022 / Revised: 07 September 2022 / Accepted: 14 October 2022

Abstract: MXenes, a newly emerging class of layered two dimensional (2D) materials, are promising solid lubricants due to their 2D structure consisting of weakly-bonded layers with a low shear strength and ability to form beneficial tribo-layers. This work aims at evaluating for the first time MXenes lubrication performance and tribofilm formation ability on different metallic substrates (mirror-lapped Fe and Cu discs). After depositing MXenes via ethanol (1 wt%) on the substrates, pronounced differences in the resulting substrate-dependent frictional evolution are observed. While MXenes are capable to reduce friction for both substrates after the full evaporation of ethanol, MXenes lubricating effect on Cu is long-lasting, with a 35-fold increased lifetime compared to Fe. Raman spectra acquired in the wear-tracks of the substrates and counter-bodies reveal notable differences in the friction-induced chemical changes depending on the substrate material. In case of Fe, the progressive failure of MXenes lubrication generates different Fe oxides on both the substrate and the ball, resulting in continuously increasing friction and a poor lubrication effect. For Cu, sliding induces the formation of a Ti_3C_2-based tribofilm on both rubbing surfaces, enabling a long-lasting lubricating effect. This work boosts further experimental and theoretical work on MXenes involved tribo-chemical processes.

Keywords: Mxenes; $Ti_3C_2T_x$; nano-sheets; coefficient of friction; Raman spectroscopy; tribochemistry

1 Introduction

Friction and wear phenomena occur in almost all moving parts/components. Their utmost importance becomes evident when considering the energy balance of passenger cars or processes in mining industry, where friction and wear account for about 33% of the entire energy losses [1–6]. To improve the systems or components efficiency, and to extend their service lifetime thus reducing maintenance, tremendous research effort has been dedicated to reduce friction and wear in the last decades.

Potential solution strategies are plentiful, ranging from the change of design concepts and materials over the usage of low-shear strength coatings, and the modification of the involved surfaces to the use of liquid lubricants (oils and greases) [7, 8]. In this regard, the application of liquid lubricants mixed with an additive package is still the easiest approach to effectively reduce the contact between rubbing surfaces thus reducing friction and diminishing wear. However, the tendency to reduce the lubricant viscosity and,

* Corresponding author: Alberto ROTA, E-mail: alberto.rota@unimore.it

therefore, the acting oil film thickness, as well as more restrictions with respect to specific additives, urgently ask for new lubrication concepts.

The usage of nanomaterials is an efficient strategy to overcome these limitations thus further improving the tribological performance of liquid lubricants [9–12]. Two-dimensional (2D) nanomaterials such as graphene and graphene oxide have shown an excellent performance as lubricant additive due to their low shear strength and nano-scroll formation, as verified for graphene [13–17]. Moreover, 2D nanomaterials have shown to be capable to induce the formation of beneficial tribolayers, which can substantially improve the resulting friction and wear performance [18–21].

With respect to 2D nanomaterials, MXene nano-sheets have recently emerged as an attractive material for tribological purposes. Being based upon MAX precursors with the general formula $M_{n+1}AX_n$ (M: early transition metal, A: element from 13–16, X: carbon and/or nitrogen and n = 1 to 4), MXenes are mainly synthesized by selectively removing the A-elements by wet etching. MXenes can be described by $M_{n+1}X_nT_x$, for which T_x resembles all potential surface terminations including –OH, –O, –F and –Cl groups depending on the etching route [22–25].

Due to MXenes theoretically predicted low shear strength, ceramic-like bonding characteristics and ability to form beneficial tribolayers, these nano-sheets have attracted significant attention in the tribological community when used as lubricant additives or solid lubricant coatings [18, 26]. In case of solid lubrication, multi-layer $Ti_3C_2T_x$ have shown an excellent performance when deposited onto copper [27], stainless steel [28–30], or silicon [31, 32] resulting a 4-fold friction reduction [27, 28]. Marian et al. [33] tested the tribological performance of multi-layer $Ti_3C_2T_x$ coatings for different relative humidities. They verified that these nano-sheets performed best under low humidity conditions, where higher relative humidities tended to increase friction. The first demonstration of superlubricity of $Ti_3C_2T_x$ coatings under solid lubrication was realized in a dry nitrogen environment [34]. Grützmacher et al. [29–32] verified an outstanding wear resistance for 100 nm thick, electro-sprayed $Ti_3C_2T_x$ coatings on stainless steel due to the formation of a wear-resistant tribo-layer. They demonstrated that multi-layer $Ti_3C_2T_x$ is capable to outperform all state-of-the art solid lubricants including graphene and MoS_2 regarding their wear resistance and durability. Inspired by these excellent friction and wear performance of $Ti_3C_2T_x$, the possibility to further tune the resulting tribological performance by the generation of hybrid nano-materials has been elucidated. In this regard, $Ti_3C_2T_x$ has been combined with graphene [34], nano-diamonds [31], and quantum dots [32], which resulted in an ultra-high wear resistance and a nearly zero wear behavior. The excellent wear performance of multi-layer $Ti_3C_2T_x$ nano-sheets makes them very promising for wear-critical, high-load machine components [35, 36]. Therefore, Marian et al. coated the raceways of thrust ball bearings [37] and roller bearings [38] with multi-layer $Ti_3C_2T_x$. Under more realistic working conditions, the nano-sheets induced an improved wear resistance and extended wear life, which was traced back to the generation of beneficial tribo-layers.

Concerning lubricant additives, $Ti_3C_2T_x$ has been used in paraffin oil, poly-(alpha)-olefins, among others [30–43]. For concentrations of about 1 wt%, a maximum friction and wear reduction of a factor 2 and 9, respectively, was observed. These effects were traced back to the formation of a beneficial tribo-layer thus reducing abrasion and deformation. Similar results have been obtained for MXene hybrids utilized as additives in oil [44, 45]. However, the usage of as-synthesized MXenes as lubricant additives in apolar liquids is critical due to their inherent hydrophilic character originating from synthesis and the resulting surface terminations. This, in turn, induces a phase separation between the hydrophilic nano-sheets and hydrophobic base oils, which downgrades the dispersion stability over time [18, 46]. A poor nano-sheets dispersion results in downgraded tribological properties, which have been well reported in literature when higher MXene concentrations were added to base oils [40–43]. A potential solution strategy is to chemically functionalize MXenes or to use the as-synthesized nano-sheets in polar solvents. Recently, $Ti_3C_2T_x$ chemically modified by tetradecylphosphonic acid showed an excellent stability in castor oil for about 7 days [43]. The modified MXenes improved the wear rate by about one order of magnitude

compared to castor oils mixed with as-synthesized nano-sheets [42]. With respect to different polar liquids, $Ti_3C_2T_x$ MXenes for water lubrication demonstrated their best performance for a weight concentration of 5 wt% with a friction and wear reduction of 20% and 48%, respectively [47]. Mixing $Ti_3C_2T_x$ nano-sheets with glycerol induced superlubricious states with a coefficient of friction (COF) of around 0.002 [48].

As outlined above, multi-layer $Ti_3C_2T_x$ nano-sheets show an excellent performance under solid lubrication. Considering their usage as lubricant additives, their hydrophilic character hinders the generation of a stable suspension in apolar base oils. However, the dispersion in polar solvents, which may be potentially used as green lubricants, becomes possible. Therefore, we dispersed multi-layer $Ti_3C_2T_x$ nano-sheets in ethanol and deposited them onto Fe and Cu substrates. The overall purpose of this work was to assess the effect of the substrate on the underlying tribo-film formation, which has not been explored and properly investigated so far.

2 Experimental

To test the influence of underlying substrate, discs made of Fe (99.98% pure) and Cu (99.985% pure) were used as substrate materials. The discs have been lapped to obtain a surface roughness of about 30 nm (Root Mean Square) and cleaned in ultrasonic bath with acetone and ethanol.

$Ti_3C_2T_x$ nano-sheets were synthetized using the following procedure. 5 g of Ti_3AlC_2-powder (Forsman Scientific Co. Ltd., Beijing, China) were immersed in 50 mL of an aqueous hydrofluoric acid solution (concentration of 40%) to generate multi-layer MXenes. The solution was magnetically stirred (speed 60 rpm) for about 24 h under ambient conditions at a temperature of 35 °C. Afterwards, the solution was centrifuged for 5 min at 3,500 rpm prior to the collection of the residue. Then, a final pH of 6 was adjusted by washing the suspension with deionized water prior to filtering and drying. Filtering was realized by vacuum-assisted filtration using a water circulating vacuum pump, for which poly-ether-sulfone was chosen as a filter membrane. Regarding drying, it was stored in a fridge for 8 h at –10 °C prior to freeze-dying it for 24 h at –60 °C (pressure below 30 Pa). An overview and magnified view of the as-synthesized nano-sheets acquired by scanning electron microscopy (SEM, FEI, Helios 600) are depicted in Figs. S1(a) and S1(b) in the Electronic Supplementary Materials (ESM), which clearly demonstrate the homogenous 2D-structure of $Ti_3C_2T_x$ nano-sheets and their micro-scale, lateral dimensions. Transmission electron microscopy (TEM) and X-ray diffraction (XRD, not shown here) confirmed a d-spacing of about 0.9 nm. Based upon a statistical analysis, the multi-layer $Ti_3C_2T_x$ nano-sheets have about 90 layers (z-direction) and present an average lateral size of about 1 μm (x-y-dimension). The full characterization of the as-synthesized $Ti_3C_2T_x$ nano-sheets can be found in Refs. [28] and [29].

Multi-layer MXenes were diluted in ethanol (1 wt% concentration) prior to be drop-casted onto the respective substrate. In this regard, ethanol is chemically inert and enables a good nano-sheets dispersion as well as a fast solvent evaporation after drop-casting. The use of ethanol-based suspensions has been already reported for other 2D materials, i.e. graphene flakes [49, 51]. Before deposition, the suspension was kept in an ultrasonic bath for at least 1 h to ensure a good dispersion of the nano-sheets.

The tribological tests were conducted using a ball-on-disc configuration using unidirectional sliding at a temperature and relative humidity range of 19°–25° and 30%–50%, respectively (Fig. S1(c) in the ESM). The counter-body was a steel AISI-440C ball with a diameter of 4 mm and an average surface roughness of 30 nm. The applied load was 1 N, which corresponds to a nominal Hertzian pressure of about 0.4 GPa. The velocity was kept constant at 0.1 m/s. The following tribological testing procedure was realized. Starting from dry, unlubricated conditions, the COF was monitored in real time. After having reached a stable COF (running-in period), different amounts of ethanol (1, 2, or 3 drops with a volume of 22 μL each) with and without MXenes were deposited on the substrates. In this regard, the measurements in presence of ethanol only served as reference measurements. After the full evaporation of ethanol, the substrate was re-lubricated with the same number of drops, volume, and quantity of MXenes suspension.

MXenes chemical evolution in the wear track on different substrates and on the tribological counter-bodies was studied by Raman spectroscopy, using a He–Ne laser with a wavelength of 632 nm. The acquisition parameters are: 5 s acquisition time, 300 m slit, 500 m hole, 1,800 g/mm grit size, and 100 repetitions. The chemical analysis was performed on both substrates (Fe and Cu) after MXenes deposition and full solvent evaporation. The chemical evolution of the nano-sheets was studied acquiring Raman spectra on the wear tracks of Fe and Cu substrates for two different conditions, namely when the lubrication effect of MXenes was still active (low COF in the frictional evolution), and when it was terminated (high COF in the frictional evolution). The same procedure was carried out for the wear scars of the balls.

3 Results and discussion

3.1 Substrate-dependent frictional evolution

The evolution of the COF measured on different substrates (Cu and Fe) for pure ethanol and $Ti_3C_2T_x$ ethanol suspension is presented in Fig. 1. The frictional evolution for 3 different tests performed on Fe substrates are summarized Fig. 1(a). As described in the Experimental section, the substrate was first lubricated with pure ethanol in different quantities (1E, 2E, and 3E stand for 1, 2, and 3 drops of ethanol, respectively). These experiments are important to assess the contribution of ethanol on the friction evolution thus serving as reference data. Once the COF had reached its steady-state value again, the surface was lubricated with $Ti_3C_2T_x$ ethanol suspensions (1MX, 2MX, and 3MX stand for the number of drops used). As can be seen, the evolution of the COF is fairly similar for all tests conducted. Under dry conditions (beginning of each test), the COF is about 0.2 and rapidly increases up to about 0.7 (running-in). The frictional signal becomes noisier over time, which can relate to some initial formation of wear debris. Once ethanol is dropped onto the Fe substrate, the COF instantaneously decreases to about 0.30. This low frictional level is kept constant for about 30–150 cycles, where the number of cycles with low friction correlates well with the quantity of ethanol applied. After ethanol full evaporation, the COF reaches a steady-state value of about 0.65, which goes hand in hand with a noisier signal, which may relate to the formation of debris. The application of MXene ethanol suspension induces different effects since the COF drops to a value of about 0.29. This low-COF lubricating effect lasts much longer and correlates well with the amount of

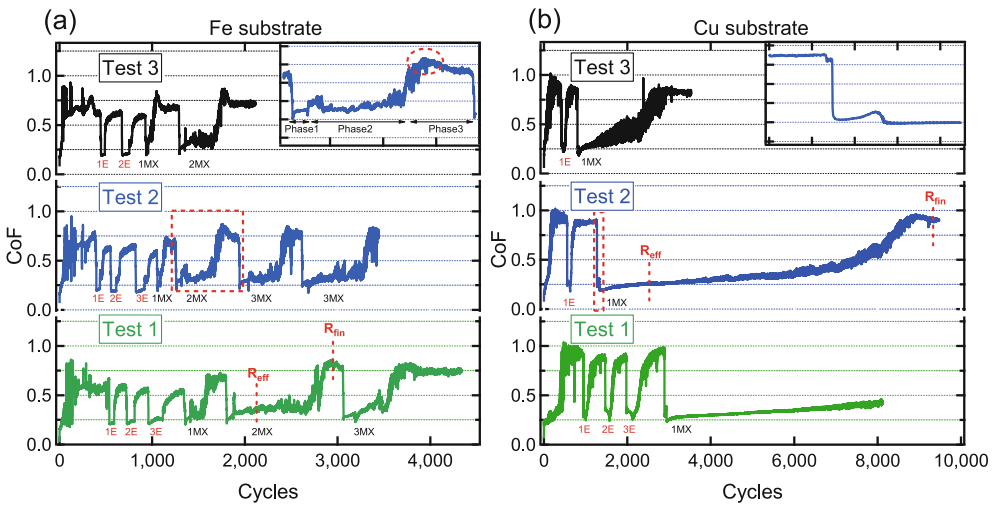

Fig. 1 Evolution of the COF measured on (a) Fe and (b) Cu substrates for pure ethanol (E) and $Ti_3C_2T_x$ ethanol suspension (MX). The respective number indicates the number of drops deposited. (a) A magnified view of the region indicated by the red-dashed rectangle in Test 2 is displayed in the inset. The red-dashed circle in the inset relates to the effect of the formed Fe oxide on the resulting COF. (b) A magnified view of test 2 of the region indicated by the red-dashed rectangle is displayed in the inset. For Test 1 and Test 2, the positions of the respective Raman measurements are highlighted by a red-dashed line labelled "R_{eff}" and "R_{fin}", which stands for "lubrication still effective" and "lubrication terminated", respectively.

MXenes applied. As demonstrated in the inset of Fig. 1(a), the effect of the MXene suspension can be divided in three phases. In the first phase, the COF is very stable with a value of 0.29. This phase can be related to the effect of ethanol, which is still present in the contact and not yet fully evaporated (phase 1). The second phase is characterized by a COF of about 0.32 and a noisier friction signal compared to the first phase. Moreover, the COF is kept low and stable for longer time lasting about 500–600 cycles in case of 3 drops applied. This phase is assigned to the lubrication effect of $Ti_3C_2T_x$ nano-sheets (phase 2). The third phase is characterized by the highest and noisiest COF with values of about 0.75 (phase 3). At the beginning of this phase before reaching steady-state conditions, the COF shows a large spike up to 0.82, which lasts for about 100–200 cycles (red dashed circle in the inset). This behavior can be related to the formation of Fe oxides, which subsequently are partially worn out, as further confirmed by Raman spectroscopy.

The evolution of the COF measured on Cu substrates for ethanol only and $Ti_3C_2T_x$ ethanol suspensions is displayed in Fig. 1(b). Initially, the COF starts at about 0.25 and ends at a value of about 0.9. Compared to Fe, a slightly different frictional behavior can be observed after the application of pure ethanol. The COF shows a fast decrease to 0.35, which is followed by a slower decrease to 0.25. Afterwards, the COF progressively increases up to values of 0.9 (noisier signal), which can be related to the evaporation of ethanol. Regarding the deposition of $Ti_3C_2T_x$ ethanol suspension, Cu substrates demonstrated notable differences in the frictional evolution compared to Fe substrates. One drop of the $Ti_3C_2T_x$ ethanol suspension is sufficient to induce a long-lasting, low and stable COF on the Cu substrate. When Cu is lubricated with 1 drop of the $Ti_3C_2T_x$ suspension, the COF instantaneously decreases to 0.2. In the very beginning, the COF shows a small peak, which lasts for about 50 cycles (inset of Fig. 1(b)). It is important to note that this peak has been reproducibly observed for all experiments with $Ti_3C_2T_x$ ethanol suspensions. Therefore, we hypothesize that this peak could be related to the nano-sheets reorientation under sliding. Afterwards, the COF remains fairly constant with a slightly increasing tendency for several 1,000 sliding cycles (1 drop of $Ti_3C_2T_x$ ethanol suspension). These results clearly demonstrate that, even after ethanol evaporation, the lubricating effect of $Ti_3C_2T_x$ survives for thousands of cycles. This is fairly different compared to the Fe substrate, which did not show similar effects even lubricated with more $Ti_3C_2T_x$ ethanol suspension. Observing the COF evolution during MXenes lubrication, it is evident that the COF becomes noisier with increasing number of cycles, which can be correlated to some debris formation. As demonstrated for different tests, the lifetime of MXenes shows some scattering. Tests 1 and 3 show a lifetime of about 7,500 and 1,750 cycles, respectively, while Test 2 shows a lifetime of more than 4,000–5,000 cycles.

Notable differences in the lubrication performance of MXenes depending on the underlying substrate are clearly shown in Fig. 1. This implies that the chemical properties of the substrate and the related chemical affinity to $Ti_3C_2T_x$ are decisive for the resulting frictional behavior. Therefore, it is essential to investigate the underlying tribo-chemical processes induced during sliding by Raman spectroscopy. In Figs. 1(a) and 1(b), the positions where the tribological test was stopped to acquire the Raman spectra are highlighted by vertical, red-dashed lines labelled as "R_{eff}" (lubrication effect still active) and "R_{fin}" (lubrication effect finished).

3.2 Analysis of the underlying tribo-chemical reactions

The Raman spectra of the $Ti_3C_2T_x$ nano-sheets after the full evaporation of ethanol on Cu and Fe substrates are summarized in Fig. 2(a). The recorded spectra on both substrates are almost identical, which indicates that the tribological experiments start with similar conditions irrespective of the substrate used. Moreover, it implies that there are no detectable interactions between the nano-sheets and substrates. The Raman peaks observed correspond to the typical Raman peaks of the material, which include a peak at about 209 cm^{-1}, a broad structure between 325 and 455 cm^{-1} and a double broad structure between 475 and 763 cm^{-1} [52]. In addition to these MXene-related features, it is possible to identify two additional peaks located at about 129 and 155 cm^{-1}. The first one relates to the use of HF during synthesis, while the second corresponds

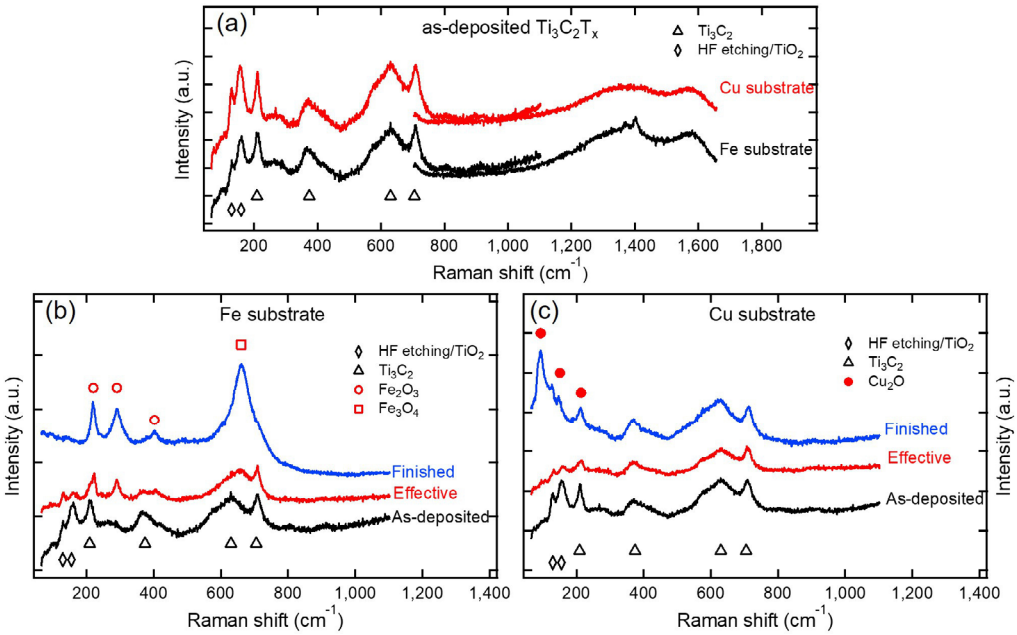

Fig. 2 (a) Raman spectra of as-deposited MXenes on Fe (black) and Cu (red) substrates after ethanol evaporation. The symbols indicate the reference peak positions for Ti_3C_2, TiO_2, and the peak related to HF etching. For technical reasons, the wavenumber range had been split in two parts to acquire the full spectrum between 53 and 1,658 cm^{-1}. (b, c) Raman spectra acquired for the wear tracks on Fe and Cu substrates, respectively. The red and blue spectra have been acquired when MXenes lubrication was still effective (R_{eff} in Figs. 1(a) and 1(b)) and terminated (R_{fin} in Figs. 1(a) and 1(b)), respectively. The black spectra correspond to the as-deposited MXenes and serve as a reference. The symbols indicate the reference peak positions for Ti_3C_2, TiO_2, and HF etching (black triangle and diamond), as well as Fe_2O_3 and Fe_3O_4 (open red circle and cube) and Cu_2O (solid red circle).

to TiO_2 [53]. The presence of TiO_2 can be connected to some superficial oxidation due to environmental oxygen and/or some synthesis-induced defects. Laser power- and acquisition time-dependent Raman measurements (not shown here) have been performed to exclude that the oxidation was induced by the Raman irradiation itself. Since the peaks located at 129 and 155 cm^{-1} also belong to and represent fingerprints of $Ti_3C_2T_x$, they have been intentionally labelled with the same color. For higher Raman shifts, another broad Raman feature between 1,100 and 1,650 cm^{-1} can be observed. This feature relates to the presence of amorphous carbon, as discussed in Refs. [54, 55]. The small peak at 1,402 cm^{-1} measured for the Fe substrate is related to the presence of Al_2O_3, which can be traced back to the used lapping solution [56].

The Raman spectra acquired on the wear tracks of the Fe and Cu substrates are summarized in Fig. 2. The Raman spectrum of the as-deposited MXene nano-sheets serves as a reference. The other two spectra have been measured at different cycles numbers of the tribological tests. To do so, the frictional test was interrupted in two distinct situations: when MXenes lubrication effect was still "effective", characterized by low COF (labelled by "R_{eff}" in Fig. 1), and when the effect of MXenes lubrication was "finished", which corresponds to high COFs in phase 3 (labelled by "R_{fin}" in Fig. 1).

In the case of Fe substrate (Fig. 2(b)), regarding the spectrum labelled with “finished”, four peaks located at 220, 290, 402, and 660 cm^{-1} can be recognized. None of these peaks can be correlated with $Ti_3C_2T_x$. Instead, they correspond to Fe oxides, i.e. α-Fe_2O_3 for the first three peaks (220, 290, 402 cm^{-1}), and Fe_3O_4 for the last peak [57]. Even though the peak at about 660 cm^{-1} could be also related to -Fe_2O_3, its symmetry points towards Fe_3O_4 [58, 59]. In contrast, the spectrum labelled “effective” shows Raman features of Fe oxides and $Ti_3C_2T_x$ nano-sheets. This agrees well with the tribological tests, for which the COF is still low thus pointing towards the lubricating effect of MXene. Further, the noisier COF signal may indicate some sliding-induced oxidation and wear debris formation,

which aligns well with the signal originating from Fe oxides.

To deepen the aspect of Fe oxidation, the Raman features related to Fe oxides have been collected after a tribological test without any lubricant (Fig. S2 in the ESM). The respective spectrum reveals Raman features corresponding to γ-Fe_2O_3 and Fe_3O_4. However, the peak at about 1,400 cm^{-1} corresponding to the γ-Fe_2O_3 is not present, contrary to the case of the MXene-lubricated surface. This difference suggests that γ-Fe_2O_3 oxide is favored by the presence of $Ti_3C_2T_x$.

The situation changes completely in case of Cu substrates, as evidenced by the Raman spectra shown in Fig. 2(c). For Cu, not only the spectrum which relates to the effective lubrication effect (labeled "effective"), but also the spectrum when lubricated effect was terminated (labelled "finished") reveals all MXene-related Raman features (black triangles and diamonds in Fig. 2(c)). In addition, the spectrum at higher Raman shifts (see Fig. S3 in the ESM.) reveals an increasing intensity of carbon features (about 1,555 cm^{-1}) during sliding. This may be connected with the release of carbon from $Ti_3C_2T_x$, contributing to the final lubricating effect. The observed MXene-related Raman features point towards the formation of a beneficial MXene-rich tribolayer. Together with the increased carbon signal, both aspects contribute to the long-lasting lubricating effect of MXene on the Cu substrate. Once MXenes lubricating effect was over ("finished"), some peaks related to CuO_2 oxide are evident at 93, 150, and 213 cm^{-1} [60]. Their presence is a confirmation that, when MXene is not able anymore to efficiently lubricate the surface, the COF returns to its pristine high value thus resulting in a pronounced oxidation of the substrate.

To deepen the understanding about the ongoing tribo-chemical processes during rubbing, the wear scars on the counter-body have been analyzed. Figure 3 depicts the optical micrographs and the related Raman analysis of the wear scar of the balls after tribological tests on the Fe and Cu substrates, which were interrupted when MXenes lubrication effect was still active.

In the case of Fe substrates (Fig. 3(a)), dark regions are visible all over the wear scar, which become larger in size and more evident towards the upper-right edge of the scar, which corresponds to the sliding direction. This dark material is well adhered to the ball and constitutes a solid film thus pointing towards a material transfer via adhesional processes. To characterize these dark areas, position-dependent Raman spectroscopy was performed, such as in the middle of the scar and on the dark-edge, as indicated in Fig. 3(a). The related spectra are displayed in Fig. 3(b) (red and green lines) and compared to the Raman spectrum obtained for the wear track on the Fe substrate

When the lubricating effect of MXenes was finished (blue line). It becomes evident that Fe_3O_4 oxides formed in the center of the scar and in the dark-edge (peak at 660 cm^{-1}). Considering that on the pristine ball the Raman signal was absent, the dark areas observed in the wear scar can be assigned to Fe oxide originating from the substrate. However, no signal of other Fe oxides (Fe_2O_3) was observed at this stage of the test. The smaller amount of dark areas in the center of the scar can be related to the competition between oxide formation and transfer, and their wearing off, while oxidic debris tends to accumulate at the scar edges. A repetition of this analysis, when the lubrication effect of MXenes was finished, evidences the appearance of the Raman peaks related to Fe_2O_3 (black line). This indicates that the presence of MXenes avoids, or at least retards, the formation of Fe oxides, which are easily formed when lubrication fails. Moreover, the evolution of the COF measured on Fe substrates shows a broad and transient increase of the COF after MXenes lubrication effect was over (inset in Fig. 1(a)). This increase prior to steady-state conditions can be related to the formation of Fe oxides once the lubrication of MXenes is over. The following decrease can be ascribed to the partial wear off of the oxides.

The situation is completely different for Cu substrates (Figs. 3(c) and 3(d)). Looking at the optical image, the center of the ball appears almost clean with some minor scratches related to sliding. Along the edge of scar corresponding to the sliding direction, a brown area is visible. This brown area seems to be an accumulation of debris that were sintered due to the high pressure and heat release during sliding (tribo-chemical reactions). The Raman spectra were

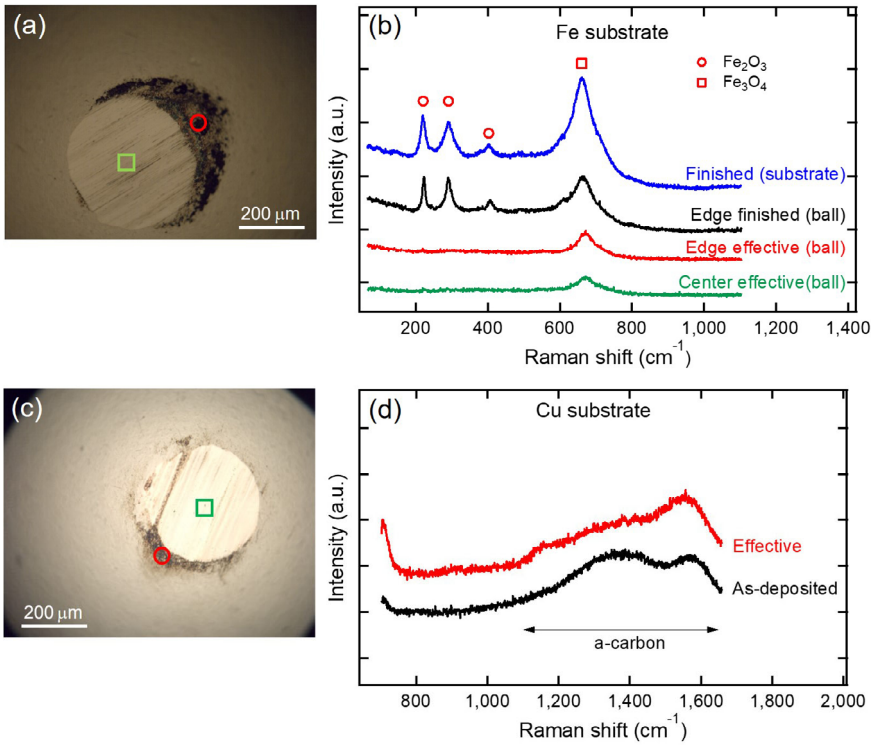

Fig. 3 (a) Optical image of the ball wear scar after a tribological test on Fe substrates lubricated with MXene suspension. The test was interrupted when the MXene effect was still effective. (b) Raman spectra acquired on the center of the ball wear scar when MXene lubrication on Fe substrate was effective (green curve), and on the edge, when lubrication was effective and finished (red and black curves), respectively. The location for which the spectra were acquired are indicated in image (a) by the green square and red circle, respectively. The spectrum acquired on the substrate wear track when the lubrication effect of MXene was over serves as a reference (blue curve). The symbols indicate the reference peak positions for Fe_2O_3 and Fe_3O_4 (red symbols). (c) Optical image of the ball wear scar after a tribological test on Cu substrate lubricated with MXene suspension. The test was interrupted when the MXene effect was still effective. (d) Raman spectra acquired on the ball wear scar in the center (green curve) and on the edge (red curve), as indicated in (c) by the green square and red circle, respectively. The spectrum acquired for the as-deposited MXenes is used as a reference (black curve). The symbols indicate the reference peak positions for Ti_3C_2, TiO_2, HF etching (dark symbols), and Cu_2O (red symbols). Prior to Raman spectroscopy, the balls were gently cleaned with ethanol to remove not-adhered wear debris.

acquired in the center of the scar and in the brown area. As comparison, the Raman spectrum of the as-deposited $Ti_3C_2T_x$ on Cu is presented (Fig. 3(d)). It is evident that the spectrum stemming from the brown edge is almost identical compared to the spectrum of the as-deposited MXenes. This means that the brown area can be considered as a transferred tribo-film consisting of $Ti_3C_2T_x$. The formation of a tribo-film in case of MXene-assisted lubrication has already been observed in literature [48, 61]. We hypothesize that this tribo-film continuously supplies self-lubricious material, maintaining friction at a low and stable level for a considerable period of time. In the related spectrum, the peaks at 192 and 162 cm^{-1}, which belong to the use of HF used for synthesis and the presence of TiO_2, respectively, are absent. The spectrum related to the center demonstrates some weak features (209 and 375 cm^{-1}), which correspond to $Ti_3C_2T_x$.

4 Conclusions

In this work, we report on the tribological behavior and the related tribo-chemical reactions of $Ti_3C_2T_x$ MXenes nano-sheets used as solid lubricants for Fe and Cu substrates. The nano-sheets have been dispersed in ethanol (1 wt%) before being drop-casted onto the substrates. The evolution of the coefficient of friction (COF) has been monitored in real-time during ball-on-discs tests to elucidate MXenes lubricating

performance depending on the used substrate. For both substrates, MXene nano-sheets are capable to reduce friction thus keeping the COF low and stable after the full evaporation of ethanol. However, this lubricating effect is much more pronounced and longer for Cu substrates, with a 35-fold increased lifetime compared to Fe substrates. To understand the origin of this notable difference, Raman spectra were acquired in the wear tracks of the substrates and counter-bodies to elucidate the friction-induced tribo-chemical reactions. Concerning Fe, the progressive failure of MXenes lubrication aligns well with the formation of Fe oxides on the wear-tracks of the substrate and counter-body. In contrast, in case of Cu, sliding induces the formation of a well-adhered Ti_3C_2-based tribofilm on both the Cu substrate and the counterbody, which induces the observed long-lasting lubricating effect. For the first time, this work clearly demonstrates that MXenes affinity to the substrate and the substrate-dependent tribo-chemical reactions decide about MXenes solid lubrication ability and performance. Apart from contributing to the fundamental knowledge about MXenes, our results aim at boosting further theoretical and experimental studies on MXenes tribochemical processes.

Acknowledgements

A. Rosenkranz gratefully acknowledges the financial support given by ANID (Chile) in the framework of the Fondecyt projects 1220331 and EQM190057. In addition, A. Rosenkranz acknowledges the support from the University of Chile and VID in the framework of U-Moderniza UM-04/19.

Electronic Supplementary Material: Supplementary material is available in the online version of this article at https://doi.org/10.1007/s40544-022-0709-3.

References

[1] Holmberg K, Erdemir A. Global impact of friction on energy consumption, economy and environment. *FME Transactions* **43**: 181–185 (2015)

[2] Holmberg K, Erdemir A. Influence of tribology on global energy consumption, costs and emissions. *Friction* **5**(3): 263–284 (2017)

[3] Holmberg K, Erdemir A. The impact of tribology on energy use and CO_2 emission globally and in combustion engine and electric cars. *Tribol Int* **135**: 389–396 (2019)

[4] Holmberg K, Kivikytö-Reponen P, Härkisaari P, Valtonen K, Erdemir A. Global energy consumption due to friction and wear in the mining industry. *Tribol Int* **115**: 116–139 (2017)

[5] Shah R, Woydt M, Huq N, Rosenkranz A. Tribology meets sustainability. *Ind Lubr Tribol* **73**(3): 430–435 (2021)

[6] Spikes H. Tribology research in the twenty-first century. *Tribol Int* **34**(12): 789–799 (2001)

[7] Myshkin N K, Goryacheva I G. Tribology: Trends in the half-century development. *J Frict Wear* **37**: 513–516 (2016)

[8] Meng Y, Xu J, Jin Z, Prakash B, Hu Y. A review of recent advances in tribology. *Friction* **8**(2): 221–300 (2020)

[9] Kumara C, Luo H, Leonard D N, Meyer H M, Qu J. Organic-modified silver nanoparticles as lubricant additives. *ACS Appl Mater Interfaces* **9**(42): 37227–37237 (2017)

[10] Cui Y, Ding M, Sui T, Zheng W, Qiao G, Yan S, Liu X. Role of nanoparticle materials as water-based lubricant additives for ceramics. *Tribol Int* **142**: 105978 (2020)

[11] Chen Y, Renner P, Liang H. Dispersion of nanoparticles in lubricating oil: A critical review. *Lubricants* **7**(1): 7 (2019)

[12] Dai W, Kheireddin B, Gao H, Liang H. Roles of nanoparticles in oil lubrication. *Tribol Int* **102**: 88–98 (2016)

[13] Liu L, Zhou M, Jin L, Li L, Mo Y, Su G, Li X, Zhu H, Tian Y. Recent advances in friction and lubrication of graphene and other 2D materials: Mechanisms and applications. *Friction* **7**(3): 199–216 (2019)

[14] Xiao H, Liu S. 2D nanomaterials as lubricant additive: A review. *Mater Des* **135**(5): 319–332 (2017)

[15] Liu L, Zhou M, Li X, Jin L, Su G, Mo Y, Li L, Zhu H, Tian Y. Research progress in application of 2D materials in liquid-phase lubrication system. *Materials* **11**(8): 1314–1330 (2018)

[16] Zhao J, Huang Y, He Y, Shi Y. Nanolubricant additives: A review. *Friction* **9**(5): 891–917 (2021)

[17] Rosenkranz A, Liu Y, Yang L, Chen L. 2D nano-materials beyond graphene: From synthesis to tribological studies. *Appl Nanosci* **10**: 3353–3388 (2020)

[18] Wyatt B C, Rosenkranz A, Anasori B. 2D MXenes: Tunable mechanical and tribological properties. *Adv Mater* **33**: 2007973–2007988 (2021)

[19] Zhang S, Ma T, Erdemir A, Li Q. Tribology of two-dimensional materials: From mechanisms to modulating strategies. *Mater Today* **26**: 67–86 (2019)

[20] Berman D, Erdemir A, Sumant A V. Approaches for achieving superlubricity in two-dimensional materials. *ACS Nano* **12**(3): 2122–2137 (2018)

[21] Berman D, Narayanan B, Cherukara M J, Berman D, Narayanan B, Cherukara M J, Sankaranarayanan S K R S, Erdemir A, Zinovev A, Sumant A V. Operando tribochemical formation of onion-like-carbon leads to macroscale superlubricity. *Nat Commun* **9**: 1164–1173 (2018)

[22] Anasori B, Lukatskaya M R, Gogotsi Y. 2D metal carbides and nitrides (MXenes) for energy storage. *Nat Rev Mater* **2**: 16098 (2017)

[23] Naguib M, Kurtoglu M, Presser V, Lu J, Niu J, Heon M, Hultman L, Gogotsi Y, Barsoum M W. Two-dimensional nanocrystals produced by exfoliation of Ti_3AlC_2. *Adv Mater* **23**: 4248–4253 (2021)

[24] Naguib M, Mochalin V N, Barsoum M W, Gogotsi Y. MXenes: A new family of two-dimensional materials. *Adv Mater* **26**(7): 992–1005 (2014)

[25] Naguib M, Barsoum M W, Gogotsi Y. Ten years of progress in the synthesis and development of MXenes. *Adv Mater* **33**(39): 2103393–2103403 (2021)

[26] Malaki M, Varma R S. Mechanotribological aspects of MXene-reinforced nanocomposites. *Adv Mater* **32**(38): 2003154–2003174 (2020)

[27] Lian W, Mai Y, Liu C, Zhang L, Li S, Jie X. Two-dimensional Ti_3C_2 coating as an emerging protective solid-lubricant for tribology. *Ceram Int* **44**: 20154 (2018)

[28] Rosenkranz A, Grützmacher P G, Espinoza R, Fuenzalida V M, Blanco E, Escalona N, Gracia F J, Villarroel R, Guo L, Kang R, Mücklich F, Suarez S, Zhang Z. Multi-layer $Ti_3C_2T_x$-nanoparticles (MXenes) as solid lubricants—Role of surface terminations and intercalated water. *Appl Surf Sci* **494**: 13–21 (2019)

[29] Grützmacher P G, Suarez S, Tolosa A, Gachot C, Song G, Wang B, Presser V, Mücklich F, Anasori B, Rosenkranz A. Superior wear-resistance of $Ti_3C_2T_x$ multilayer coatings. *ACS Nano* **15**(5): 8216–8224 (2021)

[30] Hurtado J Y A, Grützmacher P G, Henríquez J M, Zambrano D, Wang B, Rosenkranz A. Solid lubrication performance of few- and multilayer $Ti_3C_2T_x$ coatings. *Adv Eng Mater* 2200755 (2022)

[31] Yin X, Jin J, Chen X, Rosenkranz A, Luo J. Ultra-wear-resistant MXene-based composite coating via in situ formed nanostructured tribofilm. *ACS Appl Mater Interfaces* **11**(35): 32569–32576 (2019)

[32] Yin X, Jin J, Chen X, Rosenkranz A, Luo J. Interfacial nanostructure of 2D Ti_3C_2/graphene quantum dots hybrid multicoating for ultralow wear. *Adv Eng Mater* **22**: 1901369–1901381 (2020)

[33] Marian M, Song G C, Wang B, Fuenzalida V M, Krauß S, Merle B S, Tremmel S, Wartzack J, Yu J, Rosenkranz A. Effective usage of 2D MXene nanosheets as solid lubricant—Influence of contact pressure and relative humidity. *Appl Surf Sci* **531**: 147311 (2020)

[34] Huang S, Mutyala K C, Sumant A V, Mochalin V N. Achieving superlubricity with 2D transition metal carbides (MXenes) and MXene/graphene coatings. *Mater Today Adv* **9**: 100133 (2021)

[35] Marian M, Berman D, Rota A, Jackson R L, Rosenkranz A. Layered 2D nanomaterials to tailor friction and wear in machine elements—A review. *Adv Mater Interf* **9**(3): 2101622 (2022)

[36] Marian M, Berman D, Nečas D, Emani N, Ruggiero A, Rosenkranz A. Roadmap for 2D materials in biotribological/biomedical applications—A review. *Adv Colloid Interf Sci* **307**: 102747 (2022)

[37] Marian M, Tremmel S, Wartzack S, Song G, Wang B, Yu J, Rosenkranz A. Mxene nanosheets as an emerging solid lubricant for machine elements—Towards increased energy efficiency and service life. *Appl Surf Sci* **523**: 146503 (2020)

[38] Marian M, Feile K, Rothammer B, Bartz M, Wartzack S, Seynstahl A, Tremmel S, Krauß S, Merle B, Böhm T, Wang B, Wyatt B C, AnasoriB, Rosenkranz A. $Ti_3C_2T_x$ solid lubricant coatings in rolling bearings with remarkable

performance beyond state-of-the-art materials. *Appl Mater Today* **25**: 101202 (2021)

[39] Zhang X, Xue M, Yang X, Wang Z, Luo G, Huang Z, Sui X, Li C. Preparation and tribological properties of $Ti_3C_2(OH)_2$ nanosheets as additives in base oil. *RSC Adv* **5**(4): 2762–2767 (2015)

[40] Liu Y, Zhang X, Dong S, Ye Z, Wei Y. Synthesis and tribological property of $Ti_3C_2T_x$ nanosheets. *J Mater Sci* **52**(4): 2200–2209 (2016)

[41] Yang J, Chen B, Song H, Tang H, Li C. Synthesis, characterization, and tribological properties of two-dimensional Ti_3C_2. *Crystal Res Technol* **49**(11): 926–932 (2014)

[42] Feng Q, Deng F, Li K, Dou M, Zou S, Huang F. Enhancing the tribological performance of Ti_3C_2 MXene modified with tetradecylphosphonic acid. *Colloids Surf A* **625**: 126903–126914 (2021)

[43] Zhang F X, Su X, Tang G G, Xu J. Construction and tribological behaviors of MXenes/MoS_2 heterojunction with 2D/2D structure in liquid paraffin. *Chalcogenide Lett* **18**: 225–235 (2021)

[44] Zhang X, Guo Y, Li Y, Liu Y, Dong S. Preparation and tribological properties of potassium titanate–$Ti_3C_2T_x$ nanocomposites as additives in base oil. *Chinese Chem Lett* **30**(2): 502–504 (2019)

[45] Xue M, Wang Z, Yuan F, Zhang X, Wei W, Tang H, Li C. Preparation of TiO_2/$Ti_3C_2T_x$ hybrid nanocomposites and their tribological properties as base oil lubricant additives. *RSC Adv* **7**(8): 4312–4319 (2017)

[46] Malaki M, Maleki A, Varma R S. MXenes and ultrasonication. *Mater Chem A* **7**: 10843–10857 (2019)

[47] Nguyen H T, Chung K H. Assessment of tribological properties of Ti_3C_2 as a water-based lubricant additive. *Materials* **13**(23): 5545–5559 (2020)

[48] Yi S, Li J, Liu Y, Ge X, Zhang J, Luo J. *In-situ* formation of tribofilm with $Ti_3C_2T_x$ MXene nanoflakes triggers macroscale superlubricity. *Tribol Int* **154**: 106695–106704 (2021)

[49] Berman D, Erdemir A, Sumant A V. Few layer graphene to reduce wear and friction on sliding steel surfaces. *Carbon* **54**: 454–459 (2013)

[50] Berman D, Erdemir A, Sumant A V. Reduced wear and friction enabled by graphene layers on sliding steel surfaces in dry nitrogen. *Carbon* **59**: 167e175 (2013)

[51] Marchetto D, Restuccia P, Ballestrazzi A, Righi M C, Rota A, Valeri S. Surface passivation by graphene in the lubrication of iron: A comparison with bronze. *Carbon* **116**: 375–380 (2017)

[52] Wang X, Garnero C, Rochard G, Magne D, Morisset S, Hurand S, Chartier P, Rouss J, Cabioch T, Coutanceau C, Mauchamp V, Celerier S. New etching environment (FeF_3/HCl) for the synthesis of two-dimensional titanium carbide MXenes: A route towards selective reactivity vs water. *J Mater Chem A* **5**: 22012–22023 (2017)

[53] Hu T, Wang J, Zhang H, Li Z, Hu M, Wang X, Vibrational properties of Ti_3C_2 and $Ti_3C_2T_2$ (T = O, F, OH) monosheets by first-principles calculations: A comparative study. *Phys Chem Chem Phys* **17**: 9997–10003 (2015)

[54] Sarycheva A, Gogotsi Y. Raman spectroscopy analysis of structure and surface chemistry of $Ti_3C_2T_x$ MXene. *Chem Mater* **32**(8): 3480–3488 (2020)

[55] Eilers H, Kirtley J, Leichner V. Raman spectroscopy of oxygen carrier particles in harsh environments. In Proceedings of *Micro- and Nanotechnology Sensors, Systems, and Applications X,* 2018: 106390Z.

[56] Zhu Y F, Shi L, Zhang C, Yang X Z, Liang J. Preparation and properties of alumina composites modified by electric field-induced alignment of carbon nanotubes. *Appl Phys A* **89**: 761–767 (2007)

[57] Kumar P, Lee H, Kumar R. Synthesis of phase pure iron oxide polymorphs thin films and their enhanced magnetic properties. *J Mater Sci Mater Electron* **25**: 4553–4561 (2014)

[58] Dunn d S, Bogart M B, Brossia C S, Cragnolino C A. Corrosion of iron under alternating wet and dry conditions. *Corrosion* **56**: 470–481 (2020)

[59] Molchan I S, Thompson G E, Lindsay R, Skeldon P, Likodimos V, Romanos G E, Adamova G, Iliev B, Schubert T J S. Corrosion behaviour of mild steel in 1-alkyl-3-methylimidazolium tricyanomethanide ionic liquids for CO_2 capture applications. *RSC Adv* **4**: 5300 (2014)

[60] Markose K K, Shaji M, Bhatia S, Nair P R, Saji K J, Antony A, Jayaraj M K. Novel boron doped p-type Cu_2O thin film as hole selective contact in c-Si solar cell. *ACS Appl Mater Interfaces* **12**(111): 2972–12981 (2020)

[61] Gao J, Du C F, Zhang T, Zhang X, Ye Q, Liu S, W. Liu. Dialkyl dithiophosphate-functionalized $Ti_3C_2T_x$ MXene nanosheets as effective lubricant additives for antiwear and friction reduction. *ACS Appl Nano Mater* **4**(10): 11080–11087 (2021)

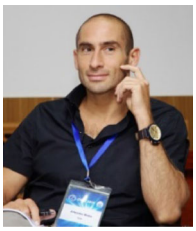

Alberto ROTA. He is an associate professor at the Department of Physics, Informatics and Mathematics of the University of Modena and Reggio Emilia, Italy. He started his carrier in surface science, focusing his activity on the chemical, structural, and morphological characterizations of extremely thin films and self-assembled nano-structures. He then moved to the tribology field, splitting his activity in basic and applied research. His main research interests are on surface patterning at the multiscale, and on 2D and solid lubricant materials (graphene, DLC, MoS_2, Ag, MXene). In particular, his activity focuses on the tribological properties and on the friction-induced chemical processes. He has pubblished more than 40 peer-reviewed journal publications and he gave more than 20 speeches in international conferences. He is a member of the Editorial Board of *Industrial Lubrication and Tribology* journal, and Review Editor for *Frontiers in Chemistry*.

Nicolas BELLINA. He graduated in physiscs at the University of Modena and Reggio Emilia, Italy, in 2020 on the deposition of DLC coating on additive manufatcured alloy for mechanical applications. He then worked as post-doctor in the same group, splitting his activity on the study of the anelastic properties of additive manufactued materials, and on the tribo-chemical properties of MXene flakes used as solid lubricant.

Bo WANG. He is a post-doctor in the Department of Materials Science & Engineering at Saarland University, Germany. He focuses his research work on the preparation and application of carbon materials including MXene, graphene, and diamond in the fields of thermal conductivity, ultra-precision machining, and tribology. He is also interested in the investigation of microstructural evolution during ultra-precision machining using transmission electron microscopy (TEM) and *in-situ* TEM. He has published more than 60 peer-reviewed journal papers and is a fellow of the Alexander von Humboldt Foundation.

Andreas ROSENKRANZ. He is a professor of materials-oriented tribology and new 2D materials in the Department of Chemical Engineering, Biotechnology and Materials at the University of Chile. His research focuses on the characterization, chemical functionalization, and application of new 2D materials. His main field of research is related to tribology (friction, wear, and energy efficiency), but he has also expanded his fields 140 water purification, catalysis, and biological properties. He has published more than 100 peer-reviewed journal publications, is a fellow of the Alexander von Humboldt Foundation and acts as a scientific editor for different well-reputed scientific journals including *Applied Nanoscience* and *Frontiers of Chemistry*.